Defect structure and superconducting properties of $La_{1.8}Sr_xCa_{1.2-x}Cu_2O_{6-\delta}$

H. Shaked,* J. D. Jorgensen, B. A. Hunter, and R. L. Hitterman
Materials Science Division, Argonne National Laboratory, Argonne, Illinois 60439

K. Kinoshita
Nippon Telegraph and Telephone Corporation Basic Research Laboratories, Musashino, Tokyo 180, Japan

F. Izumi
National Institute for Research in Inorganic Materials, 1-1 Namiki, Tsukuba, Ibaraki 305, Japan

T. Kamiyama
Institute of Materials Science, University of Tsukuba, Tsukuba, Ibaraki 305, Japan
(Received 24 March 1993; revised manuscript received 2 August 1993)

We have studied the relationship between structural defects and superconductivity in $La_{1.8}Sr_xCa_{1.2-x}Cu_2O_{6-\delta}$ ($0 \le x \le 0.8$). The samples were prepared by synthesis under different oxygen pressures, $P(O_2)=50$, 250, and 400 atm. Six of the seven samples were found to be superconducting with $22 \le T_c \le 58$ K. The structural properties were determined by neutron powder diffraction. The inter-CuO_2-plane spacing, $d_{Cu\text{-}Cu}$, increases as Ca on the $M(1)$ site between these planes is replaced by the larger Sr and La ions. The metal-site ordering is influenced by the oxygen pressure during synthesis. We have used the inter-CuO_2-plane spacing, neutron-diffraction measurements of the scattering from the metal sites, and chemical constraints to determine the occupancies of La, Sr, and Ca at the $M(1)$ site. For the same overall composition, higher oxygen pressure leads to a larger fraction of La on the $M(1)$ site. Oxygen occupancy of the vacant O(3) site in the $M(1)$ plane increases sharply when $d_{Cu\text{-}Cu}$ exceeds 3.5 Å. The superconducting transition temperature T_c decreases systematically as the occupancy of O(3) increases for samples that would otherwise be expected to be superconducting.

I. INTRODUCTION

The cuprate $La_2(Ca,Sr)Cu_2O_{6-\delta}$ was first synthesized and its crystallographic structure solved in 1980.[1] It has a tetragonal structure (Fig. 1) which belongs to the space group $I4/mmm$.[2] The structure consists of two mirror-paired CuO_2-based pyramidal layers, and layers of non-copper metals $M(1)$ (see Fig. 1) at the mirror plane and $M(2)$ at (approximately) the plane of the apical oxygen site O(2). The entire crystal is obtained from this five-layered module by repeated application of the body centering translation (Fig. 1).[3] This five-layer module (which contains two layers of CuO_2) serves as a building block in the structure of the "two-layered" high-T_c oxide superconductors.[4] For example, in $RBa_2Cu_3O_{7-\delta}$ ($T_c \approx 93$ K),[5] the structure consists of these building blocks separated by CuO "single chains," whereas in $RBa_2Cu_4O_8$ ($T_c \approx 83$ K) they are separated by "double chains."[6] In $TlCaBa_2Cu_2O_7$ ($T_c \approx 105$ K),[4,7] these building blocks are separated by a single TlO layer. In $Tl_2CaBa_2Cu_2O_8$ ($T_c \approx 108$ K) and $Bi_2CaSr_2Cu_2O_8$ ($T_c \approx 92$ K), the building blocks are separated by TlO and BiO double layers.[4,7] The first superconducting "two-layered" oxide with these building blocks and without separating planes or chains, with composition $La_{1.6}Sr_{0.4}CaCu_2O_{6-\delta}$ and with $T_c \approx 60$ K, was discovered in 1990.[8]

A transition temperature of 60 K is considerably lower than $T_c \approx 83-108$ K, which had already been found in the other two-layered cuprates. This motivated numerous studies of the different metal and oxygen compositions in this cuprate in a search of T_c higher than 60 K.[8-20] The regions of the metal-composition diagram in which these cuprates were successfully synthesized are shown in Fig.

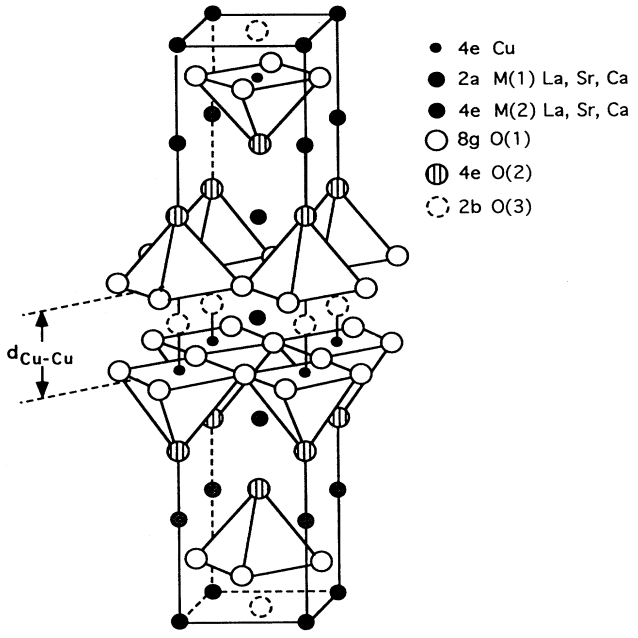

FIG. 1. Crystal structure of $La_{2-y}Sr_xCa_{1+y-x}Cu_2O_{6-\delta}$. The Wyckoff site designation (Ref. 2) is given. The O(3) site (dashed circles) is normally vacant. The inter-CuO_2-plane spacing $d_{Cu\text{-}Cu}$ is also shown.

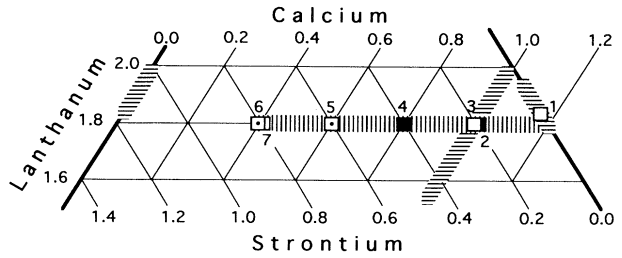

FIG. 2. Metal-composition diagram for $La_{2-y}Sr_xCa_{1+y-x}Cu_2O_{6-\delta}$. The regions in which samples were successfully synthesized are shaded: (≡) previous studies, (|||) present work. The samples which were studied in the present work are represented by square symbols and the corresponding (Table I) sample number. Open, solid, and dotted symbols represent samples synthesized at 400, 250, and 50 atm of oxygen, respectively.

2. Superconductivity was found in the Ca-rich region of the diagram. No superconductivity was found in samples with no Ca. Except for a single report of a sample with 0.5% volume of superconducting phase with T_c at ~75 K (which could be attributed to a minor phase in the sample),[20] no composition was found with T_c exceeding 60 K. Hence, at present, $La_{2-y}Sr_xCa_{1+y-x}Cu_2O_{6-\delta}$ exhibits the lowest T_c in its class of two-layered structures.

The results described above were obtained with a large number of samples with a variety of values for the adjustable parameters, which are metal composition, ordering on the two metal sites, metal-ion size, metal-ion charge (2+ or 3+), overall oxygen content, oxygen occupancy of the O(3) site between the CuO_2 planes, vacancy concentration on the O(1) site in the CuO_2 planes, excess charge (related to formal Cu valence), inter-CuO_2-plane spacing (d_{Cu-Cu}), etc. An important goal of the study of $La_{2-y}Sr_xCa_{1+y-x}Cu_2O_{6-\delta}$ is to determine which of these parameters influences superconductivity. Since the parameters are not entirely independent [for example, excess charge depends on composition, occupancy of O(3) is related to metal ordering and ion size, etc.], it is difficult to identify the controlling parameters.

In the present paper we report the results of a systematic structural study by neutron powder diffraction of a set of samples where the total metal charge is kept constant. The samples were prepared under different oxygen partial pressures along a constant La line (La=1.8, Fig. 2). The relationships between structural parameters, superconductivity, and the oxygen partial pressure at which the samples were synthesized are studied and discussed. Although it is difficult to draw unique conclusions with so many possible variables, these results, when combined with those already in the literature, provide a self-consistent picture of the relationship between defect structure and superconductivity in these compounds.

II. SAMPLE PREPARATION AND CHARACTERIZATION

Six samples of $La_{1.8}Sr_xCa_{1.2-x}Cu_2O_{6-\delta}$ were prepared and characterized at the Basic Research Laboratory of the Nippon Telegraph and Telephone Corporation (NTT). A seventh sample with the composition $La_{1.82}Ca_{1.18}Cu_2O_{6-\delta}$ prepared earlier at the same laboratory for a high-pressure experiment was included in the present study because its La content was nominally the same. The samples were synthesized with the nominal compositions listed in Table I from powders of La_2O_3, $CaCO_3$, $SrCO_3$, and CuO with purities higher than 99.9%. The synthesis[9] included hot isostatic pressing (HIP) for 100 h at 1080 °C in 20% O_2+80% Ar atmosphere. Each sample was synthesized at one of the three oxygen partial pressures: 400, 250, or 50 atm. The oxygen partial pressures used for the specific samples are listed in Table I. X-ray diffraction with Cu $K\alpha$ radiation did not show lines other than those belonging to the major phase, except for the pattern for sample No. 7, which showed weak lines not belonging to the major phase.

TABLE I. Chemical formula, oxygen pressure at which synthesized, and T_c (onset, electrical resistivity), for each of the seven samples used in the present work. NS=nonsuperconducting.

Sample No.	Chemical formula	Oxygen pressure (atm)	T_c (K)
1	$La_{1.82}Sr_{0.00}Ca_{1.18}Cu_2O_{6-\delta}$	400	52
2	$La_{1.8}Sr_{0.2}Ca_{1.0}Cu_2O_{6-\delta}$	250	56
3	$La_{1.8}Sr_{0.2}Ca_{1.0}Cu_2O_{6-\delta}$	400	58
4	$La_{1.8}Sr_{0.4}Ca_{0.8}Cu_2O_{6-\delta}$	250	51
5	$La_{1.8}Sr_{0.6}Ca_{0.6}Cu_2O_{6-\delta}$	50	42
6	$La_{1.8}Sr_{0.8}Ca_{0.4}Cu_2O_{6-\delta}$	50	22
7	$La_{1.8}Sr_{0.8}Ca_{0.4}Cu_2O_{6-\delta}$	400	NS

Electrical resistivity was measured for specimens taken from the seven samples using a standard four-probe dc method (Fig. 3). The onset transition temperatures T_c deduced from these measurements are listed in Table I. The width of the transitions [i.e., T(onset)$-T(R\approx 0)$] is 4–5 and 8–15 K for the samples synthesized at 400 atm and for the other samples, respectively.

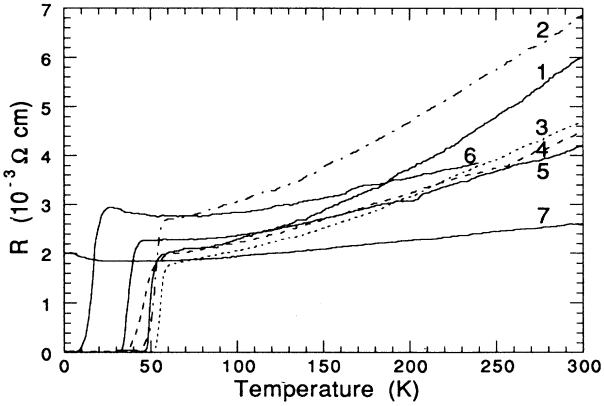

FIG. 3. Temperature dependence of the electrical resistivity for the seven samples. The sample number (Table I) is indicated for each measurement.

III. NEUTRON-POWDER-DIFFRACTION MEASUREMENTS

For the neutron-diffraction measurements, the HIP pellets (diameter $\frac{3}{4}$ in. $\times\frac{1}{8}$ in.) were broken into coarse powder. The coarse powder samples were loaded into vanadium sample holders. Neutron-diffraction data were taken for each sample at room temperature on the Special Environment Powder Diffractometer (SEPD) at the Intense Pulsed Neutron Source (IPNS).[23] Data collecting time was about 2 h, except for sample No. 1, for which it was 3 h.

The IPNS program for Rietveld analysis of the time-of-flight neutron-diffraction data[24] was used to analyze the pattern for each sample. In this analysis the structural parameters of the sample are refined so that the calculated pattern will best fit (least squares) the observed pattern. The analysis first performed assuming a single (major) phase revealed some weak reflections of a second (minor) phase in some of the samples. The minor phase reflections were found to belong to the oxygen-deficient perovskite $(La,Sr)_8Cu_8O_{20}$ (space group $P4/mbm$, lattice constants $a\approx 2\sqrt{2}a_p$, $c\approx a_p$, $a_p\approx 3.85$ Å).[25] A second two-phase analysis was consequently performed for the seven samples. The agreement factors (R_{wp}) of the two-phase analyses were lower than those of the single-phase analysis for samples Nos. 1, 3, 4, 5, and 7. It should be emphasized, however, that the amount of minor phase was sufficiently small ($\approx 2\%$ in the worst case, sample No. 4) that the refinement results were not significantly different for the single- and two-phase analyses. The tetragonal space group $I4/mmm$ was used in the analysis for the major phase. A chemical stoichiometry constraint was put on the total scattering amplitudes of the noncopper sites $M(1)$ and $M(2)$. This led to a constraint $n(1)+n(2)=\text{const}$ on the occupancies of these sites, where the constant was sample dependent (see caption of Table II and discussion in Sec. IV). Occupancies of the O(2) site, when refined, were found to be equal to unity within the statistical standard deviations and were there-

TABLE II. Structural parameters for the seven $La_{2-y}Sr_xCa_{1+y-x}Cu_2O_{6-\delta}$ samples. Rietveld refinements were done in the tetragonal $I4/mmm$ space group (Ref. 2). Atom positions are $M(1)$ at $2a$ (0,0,0), $M(2)$ at $4e$ (0,0,z), Cu at $4e$ (0,0,z), O(1) at $8g$ (0,$\frac{1}{2}$,z), O(2) at $4e$ (0,0,z) and O(3) at $2b$ (0,0,$\frac{1}{2}$) (Ref. 2). Scattering amplitudes (in units of 10^{-12} cm): 0.7719 and 0.5803 were used for Cu and O respectively (Ref. 26). An isotropic Debye-Waller factor B of 1 (Å^2) was used for O(3). n represents refined fractional occupancy; where not given $n=1$ was used. The scattering amplitudes at $M(1)$ and $M(2)$ were contrained so that $b(1)+2b(2)=0.827(2-y)+0.702x+0.49(1+y-x)$. $(La,Sr)_8Cu_8O_{20}$ was included (see text) as a second (minor) phase in the refinements of samples Nos. 1, 3, 4, 5, and 7. Numbers in parentheses are statistical errors of the last significant digit.

Sample No.		1	2	3	4	5	6	7
Chemical formula		$La_{1.82}Sr_{0.0}Ca_{1.18}Cu_2O_{6-\delta}$	$La_{1.8}Sr_{0.2}Ca_{1.0}Cu_2O_{6-\delta}$	$La_{1.8}Sr_{0.2}Ca_{1.0}Cu_2O_{6-\delta}$	$La_{1.8}Sr_{0.4}Ca_{0.8}Cu_2O_{6-\delta}$	$La_{1.8}Sr_{0.6}Ca_{0.6}Cu_2O_{6-\delta}$	$La_{1.8}Sr_{0.8}Ca_{0.4}Cu_2O_{6-\delta}$	$La_{1.8}Sr_{0.8}Ca_{0.4}Cu_2O_{6-\delta}$
O_2 pressure (atm)		400	250	400	250	50	50	400
a (Å)		3.8206(1)	3.8222(1)	3.8221(1)	3.8264(1)	3.8343(1)	3.8389(1)	3.8366(1)
c (Å)		19.4355(2)	19.5324(2)	19.5362(2)	19.6363(2)	19.7427(2)	19.8569(1)	19.8925(2)
V (Å^3)		283.698(3)	285.355(3)	285.399(3)	287.504(3)	290.248(3)	292.628(3)	292.802(3)
$M(1)$ at $2a$	b	0.502(4)	0.521(4)	0.530(4)	0.553(4)	0.613(4)	0.646(4)	0.674(4)
	B (Å^2)	0.48(4)	0.40(4)	0.37(4)	0.34(4)	0.37(4)	0.47(3)	0.76(4)
$M(2)$ at $4e$	z	0.1758(1)	0.1762(1)	0.1762(1)	0.1768(1)	0.1774(1)	0.1781(1)	0.1782(1)
	b	0.791(2)	0.799(2)	0.794(2)	0.804(2)	0.796(2)	0.800(2)	0.786(2)
	B (Å^2)	0.57(2)	0.60(2)	0.65(2)	0.69(2)	0.67(2)	0.82(2)	0.72(2)
Cu at $4e$	z	0.584 51(5)	0.585 24(5)	0.585 54(5)	0.586 57(5)	0.588 15(5)	0.598 65(5)	0.590 00(6)
	B (Å^2)	0.29(2)	0.35(2)	0.34(2)	0.40(2)	0.43(2)	0.49(1)	0.58(2)
O(1) at $8g$	z	0.082 18(5)	0.082 15(4)	0.082 11(4)	0.082 47(4)	0.082 61(4)	0.083 71(4)	0.084 74(5)
	n	0.995(4)	0.988(3)	0.993(3)	0.978(3)	0.980(3)	0.970(3)	0.983(4)
	U_{11} (Å^2)	0.0018(3)	0.0019(3)	0.0017(3)	0.0013(3)	0.0024(3)	0.0034(3)	0.0046(4)
	U_{22} (Å^2)	0.0069(4)	0.0073(3)	0.0075(3)	0.0076(3)	0.0075(3)	0.0082(3)	0.0086(4)
	U_{33} (Å^2)	0.0167(5)	0.0173(5)	0.0173(5)	0.0183(5)	0.0170(5)	0.0222(5)	0.0299(7)
O(2) at $4e$	z	0.7045(1)	0.7039(1)	0.7038(1)	0.7038(1)	0.7035(1)	0.7034(1)	0.7026(1)
	U_{11} (Å^2)	0.0277(5)	0.0278(4)	0.0284(4)	0.0286(4)	0.0312(4)	0.0327(4)	0.0318(5)
	U_{33} (Å^2)	0.0078(6)	0.0077(5)	0.0068(5)	0.0092(6)	0.0071(6)	0.0097(6)	0.0113(7)
O(3) at $2b$	n	0.015(5)	0.010(5)	0.017(5)	0.030(5)	0.007(5)	0.089(5)	0.145(5)
R_{wp} (%):		5.504	5.382	5.178	4.930	5.126	4.772	5.084
R_{expt} (%):		2.760	3.182	3.064	3.103	2.941	3.015	2.873

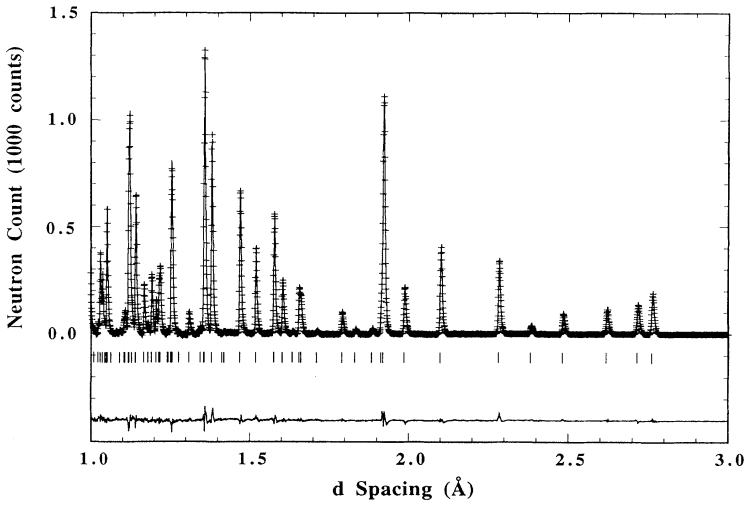

FIG. 4. Portion of the Rietveld refinement profile for sample No. 6. The plus signs (+) represent the raw time-of-flight neutron-powder-diffraction data. The solid line represents the calculated profile. Tick marks represent the positions of the allowed Bragg reflections. The background was fit as part of the refinement, but has been subtracted prior to plotting. A difference curve (observed minus calculated) is plotted at the bottom.

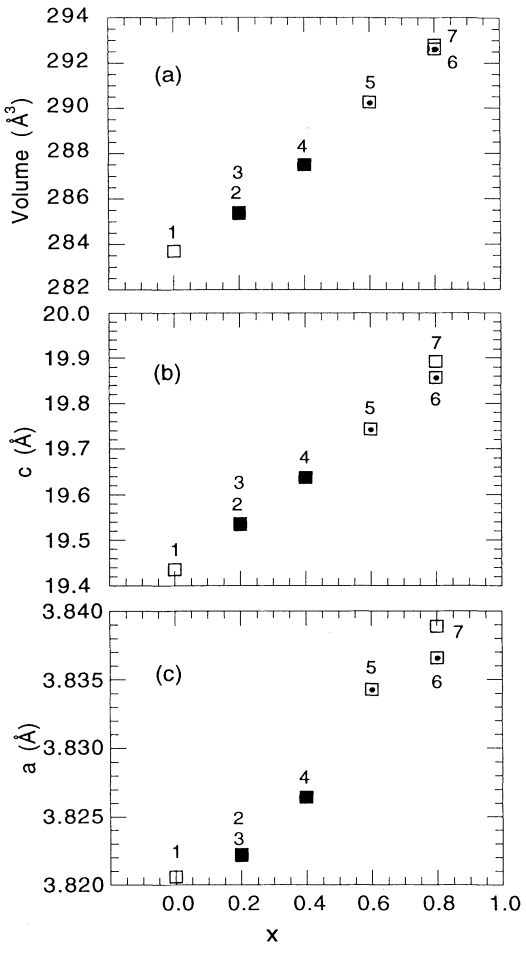

FIG. 5. Refined lattice parameters and unit-cell volume variation with the Sr content x in $La_{1.8}Sr_xCa_{1.2-x}Cu_2O_{6-\delta}$. The meaning of the symbols is the same as in Fig. 2. Error bars, taken as the statistical standard deviations from the Rietveld refinement, are smaller than the symbols and are not shown.

fore set to unity and were not refined in the reported analyses. A typical refinement included approximately 360 major phase reflections and 26 major phase variables. A typical Rietveld refined diffraction pattern (sample No. 6) is shown in Fig. 4. A summary of the results of the refinements is given in Table II.

Lattice constants and the unit-cell volume increase systematically (Fig. 5) as larger Sr ions replace the smaller Ca ions in the cuprate. However, the behavior of the lattice constants shows that the oxygen partial pressure during synthesis can also affect the structure. This is evidenced by samples Nos. 6 and 7, which have the same overall chemical composition, but were synthesized at different pressures.

Since it is impossible to determine the distribution of the three metal atoms La, Sr, and Ca on the two metal sites $M(1)$ and $M(2)$ from the neutron-diffraction data alone, we refined the scattering amplitudes for the $M(1)$ and $M(2)$ sites, assuming full occupancy. Two pairs of samples which have the same overall metal compositions ($x=0.2$ for samples Nos. 2 and 3, and $x=0.8$ for samples Nos. 6 and 7) but were synthesized at different oxygen partial pressures show differences in scattering amplitudes which indicate that the metal ordering is influenced by the synthesis pressure. Higher synthesis pressures yield systematically higher scattering amplitudes on the $M(1)$ site. The individual scattering amplitudes are $b(\mathrm{La})=0.827$, $b(\mathrm{Sr})=0.702$, and $b(\mathrm{Ca})=0.490$. Thus, from this observation, we conclude that the number of Ca ions on the $M(1)$ site that are replaced by Sr and/or La ions increases with synthesis pressure.

IV. ANALYSIS AND DISCUSSION

A. Metal ordering

The Rietveld analysis yields only the refined scattering amplitudes $b(M(1))$ and $b(M(2))$ for the two (non-copper) metal sites $M(1)$ ($2a$) and $M(2)$ ($4e$), respectively (Fig. 1). Except for sample No. 1 (which contains only

two noncopper metals), the Rietveld analysis is not capable of uniquely determining the fractional occupancies of the three (noncopper) metals on these two sites. Assuming that there are no vacancies on the $M(1)$ site, it is possible to write the following two equations for the fractional occupancies u, v, and w of La, Sr, and Ca of this site:

$$u+v+w=1 , \tag{1}$$

$$b(\mathrm{La})\cdot u+b(\mathrm{Sr})\cdot v+b(\mathrm{Ca})\cdot w=b(M(1)) , \tag{2}$$

where b(La), b(Sr), and b(Ca) are equal to 0.827, 0.702, and 0.490 (10^{-12} cm),[26] and $b(M(1))$ is equal to the refined value for the sample (Table II). The corresponding equations for $M(2)$ are not independent (see preceding section) of Eqs. (1) and (2) and yield no additional information. Only in the case of sample No. 1, which does not contain Sr and therefore $v=0$, is it possible to uniquely solve Eqs. (1) and (2) for the fractional occupancies. The authors of two previous studies[10,11] made the assumption that Sr does not occupy the $M(1)$ site and were consequently able to claim a unique solution for Sr-containing samples. Applying this assumption (i.e., $v=0$) to our data yields, for samples Nos. 4, 5, 6, and 7, Ca occupancies (w's) in excess of the samples nominal Ca content ($1.2-x$). We are therefore able to conclude that the assumption that Sr does not occupy the $M(1)$ site is inconsistent with the data of four samples of the present work and is therefore not justified. It is of interest to point out that the "converse" assumption, that La does not occupy $M(1)$, leads to a solution which is consistent within the uncertainty of the measurements with our data. But in connecting to previously published results for samples Nos. 16 and 18 (Table III), this solution requires a sharp increase (decrease) in La(Sr) occupancy as the La-Sr line (Fig. 2) is approached. Hence, until independent data supporting such an extreme behavior are presented, this solution is also excluded.

Since neither $u\equiv 0$ nor $v\equiv 0$ are acceptable, a third relation between u, v, and w, independent of Eqs. (1) and (2), is required to uniquely determine u, v, and w. Sakurai *et al.* have used x-ray diffraction in combination with neutron diffraction to obtain this third relation.[12] We argue here that the distance between the two CuO_2 planes, $d_{\mathrm{Cu\text{-}Cu}}$ (Fig. 1), can provide the additional information. Intuitively, one would expect this distance to depend on the size of the ion (Table III) that occupies the $M(1)$ site. We assume the linear relation

$$d_{\mathrm{Cu\text{-}Cu}}=uA+vB+wC , \tag{3}$$

where A, B, and C are sample-independent constants corresponding to the effective "sizes" of the La, Sr, and Ca ions at the $M(1)$ site. The observed linear increase of $b(M(1))$ (which is itself a linear function of u, v, and w), with $d_{\mathrm{Cu\text{-}Cu}}$ (Fig. 6), is consistent with such a relation. Using this model [i.e., Eq. (3)], A, B, and C were found such that

$$\sum[d_{\mathrm{Cu\text{-}Cu}}(\mathrm{obs})-d_{\mathrm{Cu\text{-}Cu}}(\mathrm{calc})]^2=\text{minimum} , \tag{4}$$

where $d_{\mathrm{Cu\text{-}Cu}}$(calc) is given by Eq. (3). The sum was evaluated for samples Nos. 1–10, 12, 13, 16, and 18 (Table IV), including the samples studied in the present work and data from the literature. Samples Nos. 11, 14, 15, and 17 from the literature were not used in this analysis because the metal occupancies reported for them were assumed and were not derived from analysis of the diffraction patterns. In seven samples, u, v, and w were fixed, since they have been uniquely determined prior to the present analysis. Six of these samples contained only two noncopper metals, and the seventh sample was uniquely solved using a combined refinement of neutrons and x rays. In the other seven samples, u, v, and w were allowed to vary, constrained by sample stoichiometry.

The values thus obtained for the constants A, B, and C were 3.67, 3.82, and 3.26 Å. These values are in qualitative agreement with the M-O (M=La,Sr,Ca) bond lengths based on the ($CN=8$) ionic radii[27] (Table III). The quality of the agreement between the calculated [Eq. (3)] and observed $d_{\mathrm{Cu\text{-}Cu}}$ is presented graphically in Fig. 7. It is believed that the poor agreement with sample No. 18 [$d_{\mathrm{Cu\text{-}Cu}}$(obs)=3.756 Å, Table IV] is due to its exceptionally high occupancy of O(3), which tends to increase $d_{\mathrm{Cu\text{-}Cu}}$(obs), an effect which was not taken into account in our model. The La, Sr, and Ca fractional occupancies of the $M(1)$ site, u, v, and w, which were obtained through the use of the present model, are shown in Fig. 8. For small x ($x<0.5$), Ca^{2+} is replaced mostly by Sr^{2+}, while for large x ($x>0.5$), a considerable increase of La^{3+} occupancy is observed.

The model used in the present analysis assumes that

TABLE III. M-O bond lengths, in Å units, based on crystal ionic radii (CR) and effective ionic radii (IR), for La^{3+}, Sr^{2+}, and Ca^{2+}, with coordination number = 8 (Ref. 27).

	CR	IR
La^{3+}	2.58	2.56
Sr^{2+}	2.68	2.66
Ca^{2+}	2.54	2.52

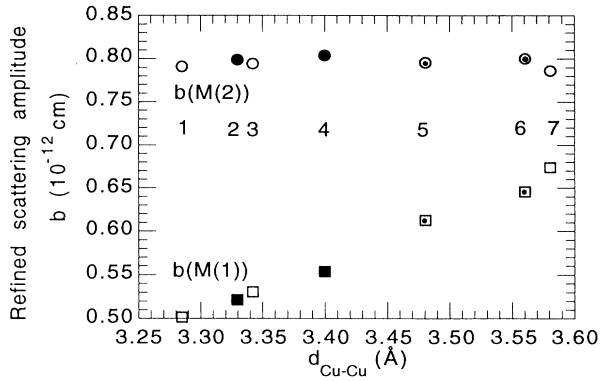

FIG. 6. Refined scattering amplitudes of the $M(1)$ (squares) and $M(2)$ (circles) sites vs the inter-CuO_2-plane spacing $d_{\mathrm{Cu\text{-}Cu}}$ (Fig. 1). The meaning of the symbols is the same as in Fig. 2. Error bars, taken as the statistical standard deviations from the Rietveld refinement, are about the same size as the symbols and are not shown.

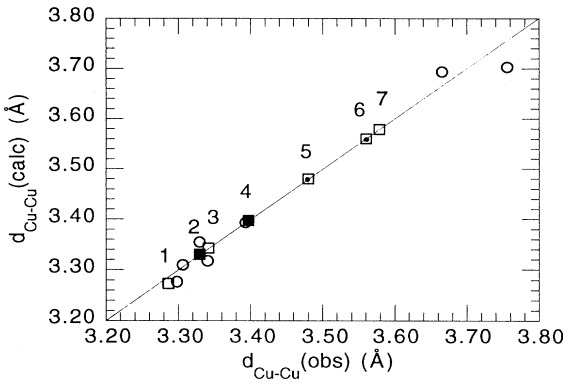

FIG. 7. Calculated vs observed inter-CuO_2-layer spacings. $d_{Cu-Cu}(calc)=3.67u+3.82v+3.26w$, where u, v, and w are the La, Sr, and Ca occupancies of the $M(1)$ site (Table IV). $d_{Cu-Cu}(obs)=[z(Cu)-0.5]c$, where z and c are the Rietveld refined values (Table II). Open, solid, and dotted squares represent samples of the present work (Nos. 1–7), synthesized at 400, 250, and 50 atm of O_2, respectively. Samples of other studies (Nos. 8, 9, 10, 12, 13, 16, and 18, Table IV) are represented by circles.

the $M(1)$ site is fully occupied [see Eqs. (1) and (2)]. In order to assess the sensitivity of the model to this assumption, we have introduced 1% vacancies to the $M(1)$ site and found that this caused (u,v,w) to vary by approximately (0.03, −0.02, −0.01). Hence, vacancies will tend to increase the La occupancy of this site.

A small enhancement is observed [Fig. 8(a)] in the La^{3+} occupancy u of the $M(1)$ site for higher oxygen synthesis pressures. Since La has the largest neutron-scattering amplitude, this result explains the increase of the scattering amplitude on $M(1)$ with synthesis pressure discussed (Sec. III) earlier. Qualitatively, this result is independent of the model (involving d_{Cu-Cu}) that was used to obtain it.

B. Oxygen occupancies

The results of the Rietveld analyses of the neutron powder data show (Table II) the existence of vacancies on the CuO_2-plane oxygen site O(1) and the incorporation of "interstitial" oxygen ions on the O(3) site (see Fig. 1) that is vacant in the ideal structure for some samples. The concentration of vacancies on O(1) generally increases with x, as shown in Fig. 9(a). However, higher oxygen partial pressure during synthesis leads to a somewhat lower vacancy concentration for the same metal composition, as would be expected. The occupancy of the interstitial site O(3), on the other hand, remains small as x is increased, until x exceeds about 0.6; then, it increases sharply, as shown in Fig. 9(b). Again, as expected, higher oxygen partial pressures lead to higher occupancies on the O(3) site.

The behavior of the O(3) site can be more easily understood when one considers the occupancy of this site as a function of the space available to accommodate the interstitial oxygen, as shown in Fig. 10. The amount of oxygen on the O(3) site increases sharply when d_{Cu-Cu} exceeds about 3.5 Å. As already discussed, this distance depends on the average size of the metal ions on $M(1)$, being larger when higher fractions of La or Sr are present

TABLE IV. Summary of $La_{2-y}Sr_xCa_{1+y-x}Cu_2O_{6-\delta}$ sample characteristics for the present work (pW) and the literature. Sample Nos. 1–10, 12, 13, 16, and 18 were used in the refinement of A,B,C in Eq. (3) (see text). The metal occupancies refer to the $M(1)$ ($2a$) site. n = neutrons and x = x rays. NS = nonsuperconducting.

No.	T_c obs. (K)	Metal stoichiomet. La/Sr/Ca	Metal $[M(1)]$ occupancies La/Sr/Ca	d_{Cu-Cu} obs. (Å)	d_{Cu-Cu} calc. (Å)	Oxyg. defic. δ	Occup. of O(3)	Expt. Technique	Ref.
1	52	1.82/0.00/1.18	0.03/0.00/0.97	3.285	3.273	0.006	0.016	n	pW
2	56	1.8/0.2/1.0	0.03/0.11/0.86	3.330	3.330	0.039	0.011	n	pW
3	58	1.8/0.2/1.0	0.05/0.11/0.84	3.342	3.342	0.014	0.017	n	pW
4	51	1.8/0.4/0.8	0.06/0.21/0.73	3.400	3.400	0.058	0.030	n	pW
5	42	1.8/0.6/0.6	0.21/0.24/0.55	3.481	3.481	0.074	0.007	n	pW
6	22	1.8/0.8/0.4	0.23/0.37/0.40	3.560	3.560	0.032	0.089	n	pW
7	NS	1.8/0.8/0.4	0.34/0.32/0.34	3.581	3.581	−0.076	0.146	n	pW
8	NS	2.0/0.0/1.0	0.23/0.00/0.77	3.330	3.354	−0.038	0.037	n	16
9	60	1.82/0.00/1.18	0.04/0.00/0.96	3.298	3.276	−0.014	0.014	n	18
10	NS	1.9/0.0/1.1	0.12/0.00/0.88	3.306	3.309			n	13
11		1.9/0.0/1.1	0.1/0.0/0.9	3.233	3.301	−0.05		x	1
12	60	1.8/0.2/1.0	0.14/0.00/0.86	3.341	3.317	−0.033	0.023	n and x	12
13	55	1.6/0.4/1.0	0.07/0.19/0.74[a]	3.393	3.393	0.06		n	10
14	NS	1.6/0.4/1.0	0.10/0.31/0.59	3.354	3.475			x	17
15		2.0/1.0/0.0	0.5/0.5/0.0	3.631	3.745	0.0		x	1
16	NS	2.0/1.0/0.0	0.84/0.16/0.00	3.665	3.694	−0.033	0.057	n	14
17		1.9/1.1/0.0	0.5/0.5/0.0	3.701	3.745	−0.05		x	1
18	NS	1.85/1.15/0.00	0.78/0.22/0.00	3.756	3.703	−0.25	0.28	n	15

[a]The authors (Ref. 10) assumed that Sr is excluded from $M(1)$ and reported 0.19/0.00/0.81. By relaxing the exclusion of Sr from $M(1)$ and requiring that $d_{Cu-Cu}(calc)=d_{Cu-Cu}(obs)$ for this sample, we have obtained the occupancies given in the table.

at the $M(1)$ site.

Although simple arguments about the size of the interstitial site O(3) may be sufficient to explain the observed behavior, it is interesting to consider the possible effects of Coulomb attraction. Samples with a significant amount of interstitial [O(3)] oxygen exhibit a correlation between the occupancy of O(3) and the amount of La^{3+} on the $M(1)$ site. This is most clearly seen for sample Nos. 6 and 7, which have the same overall metal composition, but were synthesized at 50 and 400 atm oxygen pressure, respectively [see Figs. 8(a), 9, and 10]. Sample No. 7, which contains the largest amount of O(3), also has the largest amount of La on the $M(1)$ site. This observation may explain how the synthesis pressure affects the metal ordering. High synthesis pressures result in more oxygen on the O(3) site, which increases the amount of La^{3+}, rather than Sr^{2+} or Ca^{2+}, on the $M(1)$ site by Coulomb attraction. Such an effect is evident to a lesser extent for samples Nos. 2 and 3, where $x=0.2$, but the synthesis pressures were different [see Figs. 8(a), 9, and 10]. Here, however, size effects prevent the occupancy of the O(3) site from reaching large values, and so the effect is small.

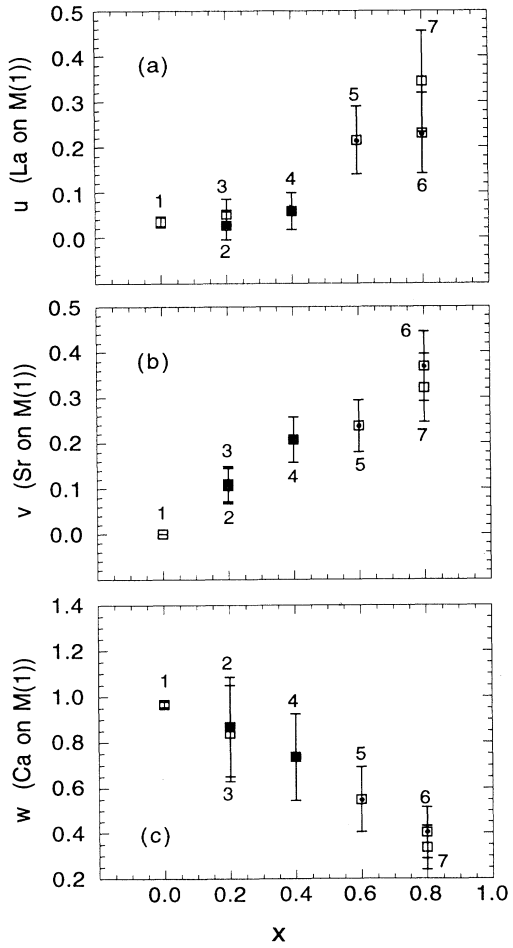

FIG. 8. x dependence of the La, Sr, and Ca fractional occupancies u, v, and w of the $M(1)$ site. The meaning of the symbols is the same as in Fig. 2.

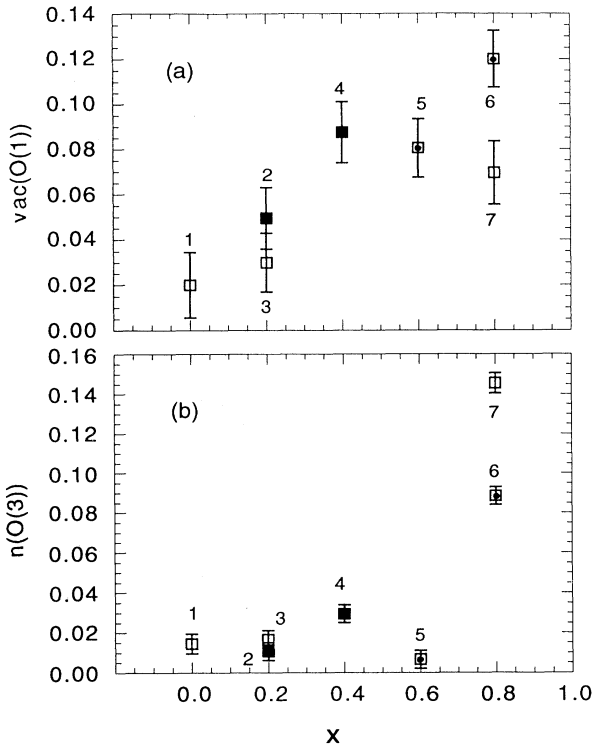

FIG. 9. (a) Number of vacancies on O(1) and (b) number of oxygen ions on O(3) per formula unit vs Sr context x. For the O(3) site, the number of oxygen atoms is equal to the fractional occupancy $n(O(3))$ since there is one O(3) site per formula unit, but for the O(1) site, $\mathrm{vac}(O(1))=4[1-n(O(1))]$, since there are four O(1) sites per formula unit. The meaning of the symbols is the same as in Fig. 2.

C. Relation to superconductivity

The occupancy of the O(3) site, $n(O(3))$, has a dramatic effect on superconductivity, as shown in Fig. 11(a). Within the accuracy of our data, T_c decreases linearly with increasing $n(O(3))$. This relation holds for all sam-

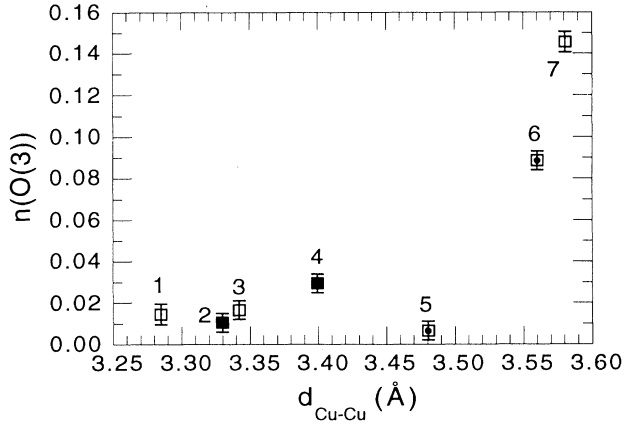

FIG. 10. Fractional occupancy of the O(3) site, $n(O(3))$, vs the inter-CuO_2-plane spacing $d_{Cu\text{-}Cu}$. The meaning of the symbols is the same as in Fig. 2.

ples studied except No. 5, whose depressed T_c can be explained on the basis of its low hole concentration (to be discussed later). As has also been noted by other authors, small concentrations of oxygen on the O(3) site (<0.04) do not destroy superconductivity. However, our results suggest that for such samples T_c may be a few degrees higher if this oxygen could be removed. Surprisingly, superconductivity does not seem to be affected by vacancies on the O(1) site, in the CuO_2 planes, up to concentrations of about 0.12 per formula unit (3%), as shown in Fig. 11(b).

The relationship of T_c to the inter-CuO_2-plane spacing $d_{\text{Cu-Cu}}$ is shown in Fig. 12(a). Superconductivity is observed over a wide range of $d_{\text{Cu-Cu}}$ values. This can be compared with the behavior of $R\text{Ba}_2\text{Cu}_3\text{O}_{7-\delta}$ compounds (R = rare earth or Y) where the $d_{\text{Cu-Cu}}$ range is small for a given compound (i.e., a given R), as oxygen content is varied. However, considering all R's, superconductivity is also sustained over a broad range of $d_{\text{Cu-Cu}}$ in these compounds. For example, $d_{\text{Cu-Cu}} \approx 3.36$ and 3.55 Å for R = Y (Ref. 21) and Nd (Ref. 22), respectively [Fig. 12(a)].

The relationship between T_c and the excess charge per Cu atom has been studied for all of the copper-oxide superconductors. In the present study, the metal compositions were chosen to provide a set of samples where this excess charge was constant except for the effects of changes in oxygen content. Although oxygen content can vary as a result of vacancies on the O(1) site or interstitials on the O(3) site, these tend to compensate one another in many samples. Thus the values for the excess charge for the samples of the present study are clustered over a small range, as shown in Fig. 12(b). When we compare our data with other data from the literature, we conclude that all of our samples lie within the region of excess charge (roughly between -0.02 and -0.2 per copper atom) where superconductivity would be expected. It is relevant to note that superconductivity is observed over a similar range of values for the excess charge in the related single-layer compound $La_{2-x}Sr_xCuO_4$.

Our sample No. 5, however, lies near the lower boundary of this region [as a result of its low occupancy of the O(3) site combined with a relatively large number of vacancies on the O(1) site]. This defect structure apparently results from the low oxygen pressure during synthesis in spite of a chemical composition that results in a rather large value for $d_{\text{Cu-Cu}}$ (providing space for some interstitial oxygen). We conclude that a low carrier concentration is the most likely explanation for the depressed T_c of

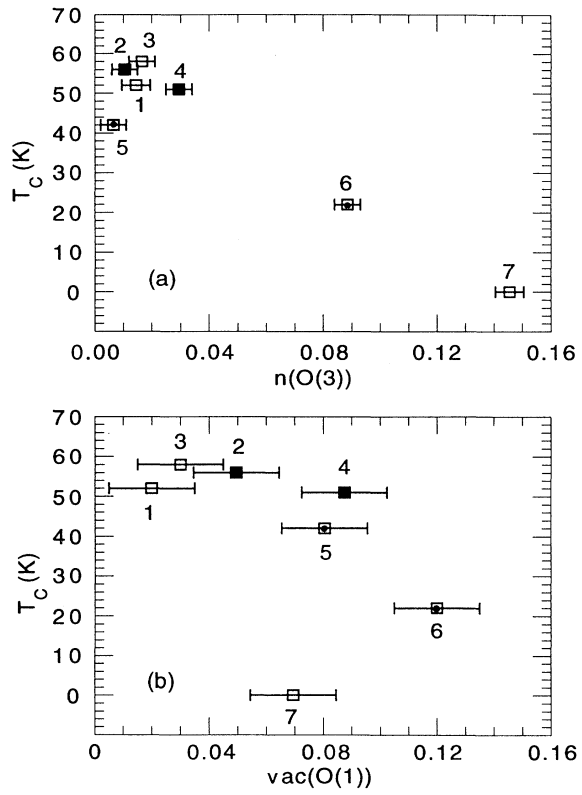

FIG. 11. (a) T_c vs number of interstitials on O(3) and (b) vs number of vacancies on O(1) per formula unit. Note that, since there are four O(1) atoms per formula unit, vac(O(1))=0.16 corresponds to 4% vacancies on this site. The meaning of the symbols is the same as in Fig. 2.

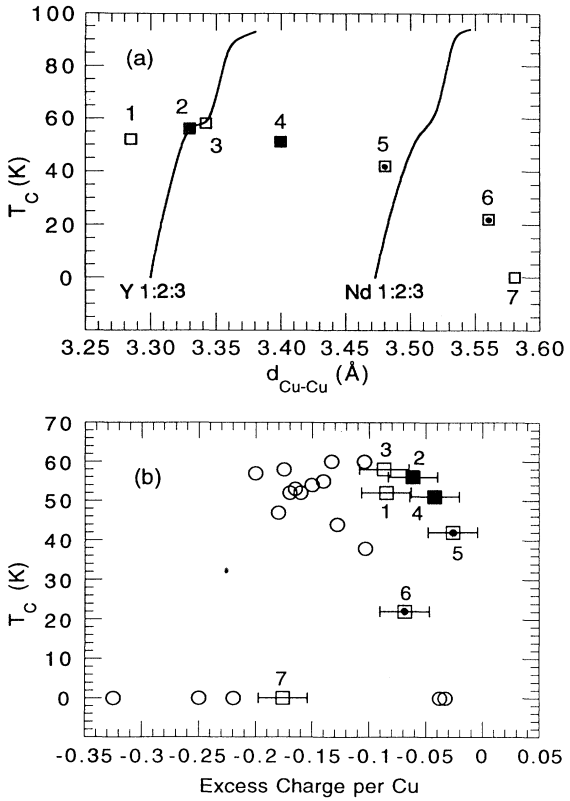

FIG. 12. (a) T_c vs the inter-CuO_2-plane spacing $d_{\text{Cu-Cu}}$. The corresponding dependencies for $R\text{Ba}_2\text{Cu}_3\text{O}_{7-\delta}$ [R = Y (Ref. 21), Nd (Ref. 22)] are shown (solid lines) for comparison. (b) T_c vs the excess charge per Cu ion in $La_{2-y}Sr_xCa_{1+y-x}Cu_2O_{6-\delta}$ ($q=\delta-y/2$), for the samples of the present work (squares) and the literature (circles) (Refs. 10, 12–18, 28, and 29). The meaning of the symbols is the same as in Fig. 2.

sample No. 5. For our other samples, the superconducting behavior can be explained solely on the basis of the defect structure.

V. CONCLUSIONS

The two-layer cuprates present a difficult challenge for determining the relationship between chemical composition, crystal structure, and superconductivity because of the large number of variables. With the limited number of samples studied here, it is impossible to draw conclusions about all of the necessary conditions for superconductivity in these compounds. However, by combining our results with those previously published, we can learn some important aspects of the behavior.

We have proposed that $d_{\text{Cu-Cu}}$ can be used to determine the La, Sr, and Ca fractional occupancies of the $M(1)$ site. Although neutron diffraction alone cannot be used to determine metal-site ordering when there are three cations (i.e., La, Sr, Ca) involved, the parameter $d_{\text{Cu-Cu}}$ can be taken as an additional observation that allows conclusions about metal-site ordering to be drawn. This procedure is performed in a way that is consistent with the samples of the present study and with samples from the published literature. Such as procedure is required to understand the defect structure, since the metal-site ordering depends on both the overall chemical composition and the oxygen partial pressure during synthesis.

The incorporation of the larger Sr^{2+} or La^{3+} ions at the $M(1)$ site between the CuO_2 planes increases the spacing $d_{\text{Cu-Cu}}$ between these planes. As a result, the incorporation of excess oxygen at the normally vacant O(3) site [in the plane of $M(1)$] increases sharply when $d_{\text{Cu-Cu}}$ becomes larger than about 3.5 Å. There is some evidence that Coulomb attraction involving these interstitial oxygen atoms enhances the amount of La^{3+} on the $M(1)$ site. Both of the oxygen-site occupancies are also influenced in the expected ways by the oxygen partial pressure during synthesis. Thus, in this way, oxygen pressure has an affect on metal-site ordering.

In the present study, the clearest effect of defect structure on superconductivity is a systematic depression of T_c as interstitial oxygen is incorporated at the O(3) site between the CuO_2 planes. This effect depresses T_c for samples which would otherwise be expected to be superconducting on the basis of their average excess charge. Surprisingly, vacancies on the O(1) oxygen site in the CuO_2 planes do not appear to depress T_c for concentrations up to about 3%.

ACKNOWLEDGMENTS

The authors wish to acknowledge helpful discussions with P. G. Radaeili, D. G. Hinks, and B. Dabrowski. This work is supported by the U.S. Department of Energy, Division of Basic Energy Sciences–Material Science, under Contract No. W-31-109-ENG-38 (J.D.J. and R.L.H.), the National Science Foundation, Science and Technology Center of Superconductivity under Grant No. DMR 91-20000 (H.S. and B.A.H.), and the Nuclear Research Center–Negev and Ben Gurion University in the Negev (H.S.).

*Permanent address: Department of Physics, Nuclear Research Center-Negev, P.O.B. 9001, Beer Sheva, Israel 84190 and Department of Physics, Ben-Gurion University of the Negev, P.O.B. 653, Beer Sheva, Israel 84105.

[1]N. Nguyen, L. Er-Racho, C. Michel, J. Choisnet, and B. Raveau, Mater. Res. Bull. **15**, 891 (1980).

[2]*International Tables for Crystallography, Vol. A: Space-Group Symmetry,* edited by T. Hahn (Kluwer Academic, Dordrecht, 1992), p. 468.

[3]This structure belongs to a family with the generic chemical formula $A_mCa_{n-1}La_2Cu_nO_{2n+m+2}$ having n-fold CuO_2 layers separated by m-fold AO layers (Ref. 4). The cuprate $La_2(Ca,Sr)Cu_2O_{6-\delta}$ having a double CuO_2 ($n=2$) layer and no separating AO layer is denoted A 0:1:2:2 in this classification.

[4]I. K. Schuller and J. D. Jorgensen, MRS Bulletin **27** (January, 1989).

[5]J. M. Tarascon, W. R. Mckinnon, L. H. Greene, G. W. Hull, and E. M. Vogel, Phys. Rev. B **36**, 226 (1987).

[6]P. Marsh, R. M. Fleming, M. L. Mandich, A. M. deSantolo, J. Kwo, M. Hong, and L. J. Martinez-Miranda, Nature **334**, 141 (1988).

[7]B. Morosin, D. S. Ginley, P. F. Hlava, M. J. Carr, R. J. Boghman, J. E. Schirber, E. L. Venturini, and J. F. Kwak, Physica C **152**, 413 (1988).

[8]R. J. Cava, B. Batlogg, R. B. van Dover, J. J. Krajewski, J. V. Waszczak, R. M. Fleming, W. F. Peck, Jr., L. W. Rupp, Jr., P. Marsh, A. C. W. P. James, and L. F. Schneemeyer, Nature **345**, 602 (1990).

[9]K. Kinoshita and T. Yamada, Phys. Rev. B **46**, 9116 (1992).

[10]R. J. Cava, A. Santoro, J. J. Krajewski, R. M. Fleming, J. V. Waszczak, W. F. Peck, Jr., and P. Marsh, Physica C **172**, 138 (1990).

[11]S. Adachi, T. Sakurai, Y. Yaegashi, H. Yamauchi, and S. Tanaka, Physica C **192**, 351 (1992).

[12]T. Sakurai, T. Yamashita, J. O. Willis, H. Yamauchi, S. Tanaka, and G. H. Kwei, Physica C **174**, 187 (1991).

[13]F. Izumi, E. Takayama-Muromachi, Y. Nakai, and H. Asano, Physica C **157**, 89 (1989).

[14]V. Caignaert, N. Nguyen, and B. Raveau, Mater. Res. Bull. **25**, 199 (1990).

[15]P. Lightfoot, Shiyou Pei, J. D. Jorgensen, X.-X. Tang, A. Manthiram, and J. B. Goodenough, Physica C **169**, 464 (1990).

[16]A. Fuertes, X. Obradors, J. M. Navarro, P. Gomez-Romero, N. Casan-Pastor, F. Perez, J. Fontcuberta, C. Miravitlles, J. Rodrigez-Carvachal, and B. Martinez, Physica C **170**, 153 (1990).

[17]S. Adachi, H. Adachi, K. Setsune, and K. Wasa, Physica C **169**, 377 (1990).

[18]K. Kinoshita, F. Izumi, T. Yamada, and H. Asano, Phys. Rev. B **45**, 5558 (1992).

[19]T. Sakurai, T. Yamashita, H. Ymauchi, and S. Tanaka, Physica C **185-189**, 601 (1991).

[20]B. Okai, Jpn. J. Appl. Phys. **30**, L179 (1991).

[21]J. D. Jorgensen, B. W. Veal, A. P. Paulikas, L. J. Nowicki, G.

W. Crabtree, H. Clauss, and W. K. Kwok, Phys. Rev. B **41**, 1863 (1990).

[22]H. Shaked, B. W. Veal, J. Faber, Jr., R. L. Hitterman, U. Balachandran, G. Tomlins, H. Shi, L. Morss, and A. P. Paulikas, Phys. Rev. B **41**, 4173 (1990).

[23]J. D. Jorgensen, J. Faber, Jr., J. M. Carpenter, R. K. Crawford, J. R. Haumann, R. L. Hitterman, R. Kleb, G. E. Ostrowski, F. J. Rotella, and T. G. Worlton, J. Appl. Crystallogr. **22**, 321 (1989).

[24]F. J. Rotella (unpublished); R. B. VonDreele, J. D. Jorgensen, and C. G. Windsor, J. Appl. Crystallogr. **15**, 581 (1982).

[25]L. Er-Rakho, C. Michel, and B. Raveau, J. Solid State Chem. **73**, 514 (1988).

[26]*International Tables for Crystallography,* Vol. C: Mathematical, Physical and Chemical Tables, edited by A. J. C. Wilson (Reidel, Dordrecht, 1983), p. 384.

[27]R. D. Shannon, Acta Crystallogr. A **32**, 751 (1976).

[28]H. B. Liu, D. E. Morris, A. P. B. Sinha, and X. X. Tang, Physica C **174**, 28 (1991).

[29]R. J. Cava, R. B. Van Dover, B. Batlogg, J. J Krajewski, L. F. Schneemeyer, T. Siegrist, B. Hessen, S. H. Chen, W. F. Peck, Jr., and L. W. Rupp, Jr., Physica C **185-189**, 180 (1991).